

TECTONICS IN GEOMORPHOLOGICAL MODELS

M. J. Kirkby

WORKING PAPER 93/10

SCHOOL OF GEOGRAPHY • UNIVERSITY OF LEEDS

WORKING PAPER 93/10

TECTONICS IN GEOMORPHOLOGICAL MODELS

M J Kirkby

**School of Geography
University of Leeds
LEEDS LS2 9JT**

TECTONICS IN GEOMORPHOLOGICAL MODELS

M.J. Kirkby, School of Geography, University of Leeds, UK

Abstract

Tectonics and process geomorphology typically operate at very different scales. We address the ways in which tectonics may be incorporated into geomorphological models at scales from 10 to 1000km. In particular we evaluate the applicability of diffusion models as an adequate approximation. At hillslope scales we have adequate physically based models to provide detailed evolutionary models. For larger areas, complete process models are generally too demanding of computer time to be applied directly, particularly in geophysical applications. Alternatively we propose that simple models may be 'stretched' in two ways. First, the whole landscape may be treated as a one-dimensional profile, dominated by river profiles. This approach is applicable to desert fan areas, such as in the Basin and Range province of the USA. Alternatively a representative mainstream profile may be linked to a set of hillslope profiles which supply it with sediment and link to it. This provides separate profiles for streams and divides, giving explicit forecasts for local relief and gradients. This method may be applied at up to continental scales, where it is relevant to combine it with isostatic/flexural and thermal effects to show the behaviour of passive continental margins.

Introduction

Although plate tectonics has been largely adopted as the dominant paradigm in earth sciences for thirty years, it has had relatively little impact on much of geomorphology. Geomorphologists have spent much of this period concentrating on small scale process and landform studies for which tectonics has minimum relevance, and have perhaps therefore found difficulty in applying their work at the regional to continental scales at which plate tectonics are most relevant.

Although the detailed conceptual models for slope evolution of W.M. Davis (1899) and Walther Penck (1924) may now appear to be largely irrelevant in the light of subsequent process based research, their work also contained implicit and explicit tectonic assumptions, and was applied by them and their followers at many landscape scales. One of the most influential commentaries on their tectonic views is Schumm's 1963 paper on rates of denudation and orogeny. He concluded that rates of active tectonic uplift are generally well in excess of regional denudation rates, so that Davis' assumption, of rapid uplift and long periods of stability, was a better first approximation than Penck's assumption of a dynamic balance between uplift and erosion. More recently, there has been an increasing preference for a Penckian dynamic balance between uplift and downcutting (eg. Adams, 1985). It has been suggested that rates might be in balance at the extremes of 25mm.a^{-1} found in the New Zealand Alps, and for relatively stable areas, such as S.E. England, at rates as low as 0.01mm.a^{-1} .

Working at large scales, geophysicists have frequently adopted a diffusion model for landscape evolution, which is related both to some sediment transport laws and to the influential generalisation of Ahnert (1970), in which denudation rates are directly linked to elevation. It is argued below that a diffusion model, suitably applied, is an adequate asymptotic model for landscape behaviour. Although less suitable for the highly transient situations which arise in response to individual tectonic events, it may be broadly applicable where tectonic activity continues for time spans which are long compared to landscape relaxation times, so that a near equilibrium can be achieved.

In this paper it is argued from a modelling standpoint that some of the process

experience acquired from local scale studies may still be effectively applied at large scales. There is then scope to improve the geomorphological content of geophysical models, and give geomorphologists back the freedom to explore a new understanding of regional to continental landscapes.

Diffusive and non-diffusive processes

Simulation models for hillslope evolution are commonly based on a continuity equation, combined with a process law for sediment transport in terms of area drained (related to flow discharges) and gradient (Kirkby, 1971). These formulations are appropriate, in their simplest form, where sediment transport is at the transporting capacity of the process (Transport or Flux limited models), and are usually associated with processes such as soil creep, solifluxion, rainsplash and inter-rill or rill-wash. Other processes are constrained by the supply of material, commonly through weathering (Weathering or Supply limited models). This approach is more appropriate for denudation by rapid mass movements (even where they are approximated as a continuous process) and by solution. It is possible (Kirkby, 1992) to combine these two approaches into a single continuum, in which mean travel distance is large (compared to the slope length of interest) for supply limited processes, and small for flux limited processes.

Strictly diffusive models are appropriate only for flux limited processes in which sediment transport is directly proportional to gradient. These are thought to be soil creep, solifluxion and rainsplash, and are generally measured as having the rather low transport rates of 10^{-3} to $10^{-2} \text{ m}^2 \cdot \text{a}^{-1}$ per unit gradient.

For the one-dimensional slope profile, and assuming no aerial sediment input, continuity dictates:

$$\frac{\partial z}{\partial t} = U - \frac{\partial S}{\partial x} \quad (1)$$

where z is elevation,

x is horizontal distance from divide,

U is the rate of tectonic uplift

S is sediment transport and

t is elapsed time.

Using the erosion limited generalisation, the transporting capacity, C , is defined as the product of a detachment rate, D and a travel distance, h . A sedimentation balance then gives:

$$\frac{dS}{dx} = D - \frac{S}{h} \quad (2)$$

where the difference between dS/dx and $\partial S/\partial x$ may be ignored except for transient cases.

With reasonable generality, the detachment rate and travel distance may be expressed as functions of distance and gradient, Λ , as in the following simple examples:

(i) Creep or Splash:

D constant

$h \propto \Lambda$

(ii) Inter-rill Wash:

D constant

$h \propto x$

(iii) Rill-wash, and by extension fluvial transport:

$D \propto (x\Lambda - \Theta_c)$ above threshold Θ_c .

$h \propto x$

(iv) Landslides:

$D \propto (\Lambda - \Lambda_0)/\Lambda$ where $S \geq 0$

$h \propto \Lambda/(\Lambda_r - \Lambda)$ where positive, ∞ elsewhere

(v) Solution:

D constant

$h \rightarrow \infty$

Together with initial and boundary conditions, such sets of equations form a basis for generating numerical simulations over time. Figure 1 (a)-(c) shows three examples, which differ only in the (constant) rate of downcutting applied at the slope base. The assumed processes follow the forms above, and include components of all five processes. For the reasonable values used, inter-rill wash is nowhere dominant and there is a zero threshold for rillwash. The initial form consists of a gently sloping plateau, with a deep incision to the slope base.

In Figure 1(a), with a fixed basal elevation, the initial evolution for about 50Ka is dominated by landslides, while the steepest part of the profile is above the threshold gradient (22° or 40%). For longer times, the plateau is steadily lowered by solution, while splash and rillwash processes generate a convexo-concave profile which gradually encroaches on the divide and lowers the whole slope, though at much lower rates than for landslides. From about 500Ka, when 80% of the initial relief still remains, the slope appears to be undergoing a general Davisian decline in relief and gradients without appreciable change in form. The extent of the concavity is slight here, but is accentuated if greater emphasis is given to downslope grainsize sorting.

In Figures 1 (b) and (c), with 0.05 and 0.10 mm a^{-1} respectively, the initial evolution is very similar, since total basal downcutting amounts to only 2.5–5m in 50Ka, but for long time spans, the profile shows elements of parallel retreat until the summit plateau has been consumed, and finally approaches a steady state form of constant lowering, in equilibrium with the rate of basal downcutting. At the lower rate of downcutting, the profile remains convex throughout, but at the higher rate the steady state form has a substantial straight section, slightly steeper than the 40% landslide threshold.

Although not shown in Figure 1, the stability of the hillslope to small perturbations can be calculated for one dimensional profiles, using Smith and Bretherton's (1972) criterion for stability; $\partial S / \partial x < S/x$, where the differentiation is performed keeping gradient constant. Instability is likely to be exhibited through enlargement of small rills to permanent tributary valleys, a process which determines the actual length of hillslopes and the drainage density of the landscape (Beven and Kirkby, 1993).

Characteristic forms and steady state profiles

It has been shown (Kirkby, 1971) that hillslopes dominated by supply limited processes tend to asymptotic forms, provided that the slope base elevation remains constant, or declines exponentially at an appropriate rate. The 'characteristic form' is one in which denudation at every point is proportional to its elevation above some base level ($-dz/dt \propto z$). Where the slope base itself is held at a fixed elevation, then this elevation is the base level. Characteristic forms also apply where the slope base itself also declines towards some base level elevation. These behaviours are closely analogous to a Davisian view of peneplanation.

Strict parallel retreat ($-dz/dt \propto \Lambda$) and constant downcutting ($-dz/dt$ constant) can occur for any of these processes. Substitution of these conditions into the equations above provides first order differential equations which normally lead to physically meaningful solutions. Constant downcutting forms, and their variations, seem particularly relevant to interpreting landforms in relation to tectonics, since plate tectonic activity commonly occurs for periods which are long compared to geomorphological evolution. Every point on the steady state profile is downcutting at the same uniform rate, corresponding closely to Hack's (1960) concept of dynamic equilibrium. There may also be conditions which show at least partial conformity with conditions of parallel retreat associated with Penck, where the slope form is retreating laterally at a uniform rate as a kinematic wave. This equilibrium state is limited by the meeting of divides, and by the extension of flux limited debris aprons on the lower parts of the hillsides, unless the slope retreat rate is matched by equivalent stream or coastal retreat.

Strictly Davisian decline ($-dz/dt \propto z$) is reached for conditions where h is negligibly small, and the transport capacity, $C = Dh$, is directly proportional to gradient and some well behaved function of distance from the divide (x). This is a fair approximation for creep, solifluxion, splash, and wash processes where there is a negligible threshold (θ_c) for grain movement. Where travel distances and/or thresholds are significant, no characteristic form solution exists, so that it is not appropriate where rillwash with a significant threshold, landslides or solution play a major part in the landscape evolution.

Figure 1 illustrates the extent to which these examples of slope profile evolution approximate to characteristic forms. The two auxiliary curves, labelled as 'Mean Elevation' and 'Relative denudation', both have a horizontal scale which is the ratio of current profile mean relief (above the current slope base) to current profile summit relief. This ratio is scaled so that 100% corresponds to the total slope length for the slope profiles. For 'Mean elevation', the vertical scale is the current mean relief for the profile, to the same vertical scale as the slope profiles. Initially the curve for mean elevation descends along the diagonal of the figure, since summit elevation is initially almost totally unaffected by erosion. As the summit begins to be eroded, the curve falls below the diagonal line. If the profile evolves towards a characteristic form, then eventually the elevation ratio on the x-axis tends to a constant value, and the curve then drops vertically. This may be seen to occur at long times in figure 1(a), where a close approximation to a characteristic form develops (limited only by the presence of a low rate of solution). In (b) & (c), convergence on a steady state requires that the curve converges on a single point, corresponding to the geometry of the steady state form.

For the 'Relative denudation' curve in figure 1, the vertical axis is the ratio of mean denudation rate to mean profile relief, in units of a^{-1} , which is shown as a logarithmic scale on the right of the figure. For a characteristic form, this ratio should tend towards a fixed value, so that the curve converges on a single point. For any steady state form, it is clear that this curve must also converge on a fixed point corresponding to the fixed slope geometry, as may be seen in (b) and (c).

In the early stages of slope evolution, it is clear that there is considerable departures from characteristic forms, as shown by the profiles themselves or the summary curves. Thus the characteristic form is a very poor approximation for landscape response to transient conditions. For the reasonable example process rates used in figure 1, it may be seen that such transient conditions persist for periods of $10^5 - 10^6$ years. At longer time periods, both true characteristic forms (Figure 1a), or steady state forms (b & c) can be treated as characteristic forms in the sense that relative denudation tends to a constant value, for the given conditions. It must be noted, however, that the constant value depends on the conditions. Figure 2 shows relative denudation expressed in terms of steady state basal downcutting rates. It might equally be expressed in terms of mean or maximum slope gradient, but shows a very great sensitivity to small changes in gradient when the maximum gradients exceed the relevant landslide threshold. This approach has the advantage of combining steady states and true characteristic forms using a single index parameter.

For steady downcutting in balance with tectonic uplift the simplest appropriate model is of uniform downcutting, again after a transient period of $10^5 - 10^6$ a. The appropriate form can be obtained, either numerically or analytically by solving equations (1) globally, and (2) separately for each applicable process. Figure 3 shows some examples, for a combination of creep/splash and landslides. The profiles are expressed as logarithmic plots of gradient against horizontal distance, for a range of steady downcutting rates.

Scaling up to larger areas

It is possible to use detailed two dimensional process models for areas ranging from small catchments to continental areas, by extending the one dimensional models described above, and including stream transport processes. This is a valuable approach, particularly in the context of determining drainage densities, and there are a number of examples of successful models for small areas, for example those of Wilgoose et al (1991). In the context of relationships with tectonics, however, the amount of computer time required is generally disproportionate to other aspects of the problem. Instead we initially require methods for averaging along one dimensional sections across the landscape.

In any analysis of larger areas, it is of first importance to add stream processes to the slope processes described above. This is generally done by extending the equations for rill wash, usually with higher exponents of distance (or area) and, in many case, gradient as well. Along major stream courses, it may be argued that landslides and solution are relatively less important, so that Sediment transport can be approximated as flux limited, at rate proportional to $(x/u)^n$, for a suitable exponent n .

Two methods are proposed to apply essentially one-dimensional models to larger areas. The first of these (the envelope profile) is to average across the entire landscape, generally referred to average elevations, or to an envelope of the range. The second method (the stream/slope profile) is to combine the branches of the stream network together into an averaged mainstream profile, dynamically linked to a sequence of one-dimensional hillslope profiles which supply sediment to the stream, and are influenced at their base by rates of stream downcutting or aggradation.

The envelope profile method provides some suggestions for the use of characteristic forms, as the simplest possible diffusion approximation. The method is also applied to an area of extensional tectonics in the Basin and Range area of Nevada. The stream/ slope approach is applied at a continental scale, first without any tectonic response, and then to an area with isostatic response and elastic flexure, on a similar scale to Southern Africa.

Envelope profiles

Using the first method, the envelope profile curve near the range divide will be dominated by interfluvial behaviour. Downstream, interfluvies tend to follow the profiles of their adjacent streams, generally with diminishing relative relief, so that the envelope profile is increasingly dominated by the stream profiles. To give proper weight to the interfluvies, it is proposed that an adequate overall profile can be modelled with a composite process law of the form:

$$S = k\Lambda \left[1 + \left(\frac{x}{u} \right)^m \right] \quad (3)$$

where k , u , m are empirical constants.

The effect of flow convergence in the catchment may be to increase the exponent m , whereas it should decrease through flow divergence in alluvial fans. Downstream fining of bed material should also increase m . In semi-arid areas, loss of discharge, through percolation into the stream bed outside the storm area,

will substantially decrease m . The appropriate value for the exponent m will therefore generally be obtained empirically, but may be expected to lie between 1.0 and 3.0. Alternatively some of these effects might be incorporated within a more explicit model.

Under constant downcutting in balance with uplift at rate T , the steady state form of the profile is given by:

$$\Lambda = T/k \times [1 + (x/u)^m],$$

which is a convexo-concave profile with its maximum gradient at

$$x = (m-1)^{1/m} u.$$

Characteristic form profiles show a similar convexo-concave form, though with a slightly narrower convexity. In both cases the overall profile is dominated by a stream profile, which shows an overall downstream reduction in gradient as $x^{(1-m)}$. The appropriate choice of m is set by this concavity, while u is associated with the breadth of the summit convexities, and k is the primary rate constant.

Characteristic forms as a first order diffusion model

It will be noted that an expression of the form of equation (3) leads to characteristic forms for the profile as a whole where base level remains fixed over time. As a result, the conclusions described above, for slope profiles, are valid for these larger regional profiles. Approximately, the constant β , in the characteristic form expression $-dz/dt = \beta z$, is given by:

$$S \approx k \Lambda (x/u)^m \approx \beta h x$$

$$\Lambda \approx h / x$$

where h is the mean basin relief.

Rearranging, we have approximately:

$$\beta \approx k/x^2 (x/u)^m$$

It may be seen that if m is close to 2, then the value of β is insensitive to the size of the catchment area, but strongly dependent on the value of u in particular. This is linked to average hillslope length and drainage density by arguments about the stability of hillslope length, and appears to lead to the conclusion that values of β should be most sensitive to climatic and lithological factors, with highest values for semi arid areas.

It is relevant to compare these conclusions with Ahnert's (1970) relationship, in which rates of denudation calculated from basin sediment yields are found to be proportional either to total elevation or to local relief. This may be viewed as a basin-scale generalisation of the characteristic form. It may be argued that, if individual slope profiles approach characteristic forms, then the entire drainage basin, which is an aggregate of profiles with common highest and lowest points, must also tend towards a characteristic form. In this asymptotic characteristic form, the rate of denudation at every point is proportional to its elevation, internal drainage lines are fixed in plan, and contour lines are also fixed in plan, though changing in elevation value over time.

If it is assumed that characteristic forms have been attained, rates of lowering are directly proportional to local mean elevations. This approach has been widely applied by geophysicists and others for its computational simplicity, but it should be recognised that the implicit assumptions are frequently not met. The characteristic form assumes first that the asymptotic approximation is valid, or in other words that the landscape is 'mature' in relation to a stable base level, and second that the appropriate hillslope and channel processes are dominant. In a tectonically active area, neither of these conditions is likely to be met. Instead,

landforms are transient or reacting to constant rates of uplift, and the steep slopes generated are undergoing rapid mass movements which are likely to be the dominant processes, at least in headwater areas. Nevertheless, it may still be possible to use the characteristic form model to represent steady state conditions, provided that it is recognised that the relative denudation rate, β , responds to hillslope gradients, and is therefore ultimately dependent on uplift rate, as was shown above for hillslopes in figure 2.

If the characteristic form method is adopted, the evolution of a landscape, or any point on it, is readily seen. In the simplest case, for denudation at rate $-dz/dt = \beta z$, and uplift at constant rate T , we have:

$$\begin{aligned} \frac{dz}{dt} &= T - \beta z \\ z &= \frac{T}{\beta} [1 - \exp(-\beta t)] \end{aligned} \quad (4)$$

where the solution assumes that $z=0$ at $t=0$.

Thus, for these constant uplift conditions, the landscape equilibrates at elevation T/β , with a response time scaled to $1/\beta$. For Ahnert's data set, the value of $1/\beta$ is approximately 10^7 years, corresponding to geological estimates of 10–50 Ma as the period required for peneplanation. Using the same value of β , Himalayan elevations (6000 m) would be in balance with uplift rates of 0.6 mm.a^{-1} , while the English Weald (200m) requires uplift of only 0.02 mm.a^{-1} .

Comparison with actual uplift rates suggests that higher β values, and therefore shorter response times, may be appropriate for higher, and therefore generally steeper, mountains. Figure 2 suggests that, at high uplift rates, the value of β increases almost linearly with the uplift rate (for a given value of u and therefore, implicitly climate). Thus if we approximate $\beta = T/L_0$, for $L_0 = 5000\text{m}$, it follows that all areas of steady uplift will ultimately reach an elevation of $L_0 = 5000\text{m}$, and that the uplift rate will only influence the time taken to reach this height. Thus at $T = 0.1 \text{ mm a}^{-1}$, the time is scaled to $L_0/T = 50 \text{ Ma}$, and for $T = 10 \text{ mm a}^{-1}$, the time required falls to 0.5 Ma . For a maritime climate, like that of the Southern Alps, it may be argued that β is also very strongly influenced directly by elevation, due to strong orographic rainfall effects.

There is thus some scope for using a diffusion model based on the characteristic form assumption to represent the responses to long continued steady uplift. It is argued however, that there is scope to refine the values of the characteristic constant, β to allow for a number of effects. The most important of these is that β increases strongly with uplift rates, though with a lower limit. β also appears to respond to climate, with higher values for semi arid than for temperate climates. These effects are sketched in Figure 4. Finally β responds directly to elevation, through orographic rainfall effects which are strongest for maritime climates (i.e. West coasts in the northern hemisphere and east coasts in the southern), and for the margins of other major mountain masses which preferentially catch precipitation.

Basin and Range tectonics

In an area of crustal extension, the movement is commonly taken up in a series of sub-parallel normal faults, which typically dip at about 60° (Jackson et al, 1988). To maintain overall geometry, blocks rotate backwards as indicated in the upper part of Figure 5. This geometry is applied here to the Basin and Range area of Nevada, which is a continental area of largely internal drainage. The uplifted footwall blocks

undergo erosion, providing material which partly covers the hanging wall block with alluvial fan deposits. In the Central Nevada Seismic Belt, alluvial fan deposits lie on basalts of 10–15Ma age, which also outcrop locally on uplifted footwalls. Extensional faulting has been accompanied by erosion over this period, and may now be approaching a dynamic equilibrium in which uplift or downwarping exactly balance erosion or deposition. Over the basin widths of 20–40km, isostatic responses are assumed uniform, and therefore ignored for this closed basin context. The centre curve in Figure 5 sketches the equilibrium form, and the lower part of the diagram indicates the spatially varying constant rates of tectonics and erosion/deposition.

Using parameter values obtained by back-analysis of the landforms of the Clan Alpine Range, an approximate dynamic equilibrium form may be derived, and is shown in figure 7. The profile is plotted as slope gradient against distance from the divide. The required boundary conditions are (i) that elevations are equal to left and right of the divide (i.e. the areas under the left and right parts of the gradient curve are equal), (ii) that the rate of change of gradient is the same on both sides of the basin axis (i.e. at the zero gradient points at far left and far right) and (iii) that gradient is continuous, though not necessarily changing smoothly, at the fault line. In the analysis shown, the effect of stretching has been ignored, as this prevents the achievement of a true equilibrium.

The resulting form shows some asymmetry about the divide, with shorter and steeper slopes on the faulted side of the range. Although the range divide is initially at the hanging wall side of the fault line, slope retreat forces some lateral migration, so that the final range asymmetry is relatively slight. The fault line is not expressed as a surface discontinuity, but appears to follow the locus of steepest slopes on one side of the range. This will not necessarily be the range front contact between bedrock and alluvial fans, because progressive erosion and deposition continuously increases the volume of sediments, which gradually bury the bedrock more and more. After long times, therefore, the fault line will outcrop well within the fan deposits.

Figure 7 shows a time-bound simulation for the same area, taking full account of basin stretching as well as faulting and rotation effects as above. The landform profile is assumed to be indefinitely repeated at left and right, so that the extreme left and right of the profiles may be joined together. The curves here show isochronous sedimentary layers within the fan deposits. The effect of back rotation can be seen in the strong asymmetry of the basin fill, with the lowest point off successive layers closely hugging the footwall slope. As for the equilibrium profile in Figure 6, the time-bound model indicates that the highly asymmetric faulting process leads to only modest asymmetry in the form of the bedrock mountain ranges:

The surface and subsurface forms are in broad agreement with the present topography and alluvial stratigraphy (Kirkby et al, in press). Although isostatic

flexure has been ignored here, due to the short basin wavelength, it is recognised that the elastic lithosphere is very thin in this area, and there may be significant small effects, perhaps associated with the generation of range-front faulting and folding on both sides of the valleys, and associated with current seismic activity.

Stream/slope profiles

The proposed alternative to the envelope curve is the use of a single stream profile which follows the lowest flow line in the landscape, representing the major river(s). At successive points along the river course, its profile is linked to a hillslope profile. The two profiles are dynamically linked through the base of the hillslope. Changes in river elevation influence slope base gradient and therefore sediment delivery. Hillslope erosion provides sediment which the river must carry, with consequences for its incision or aggradation. The hillslope divides, which are assumed symmetrical, are lowered by erosion to give summit elevations and typical slope gradients. In this approach it is thus possible to separately simulate the behaviour of stream and summit elevations. At a fault line, for example, the response to uplift may be seen in a rapid adjustment of stream elevations, but a much slower response by summits, so that local relief and local gradients are initially increased. As we will see below, flexure along passive continental margins can similarly lead to streams which cut down in response to uplift, leaving fringing mountain ranges and steep escarpments.

Stream profiles are viewed as strongly dominated by flow processes, so that an equation similar to (3) above is appropriate, with appropriate corrections to allow for the stream network and valley floor geometry. For the slope processes, however, there is no difficulty in applying the full range of both flux limited and supply limited processes, as illustrated in Table 1 above.

Linkage between slope and stream profiles is formally obtained through extension of the one dimensional continuity equation (1 above) for a valley bottom of width w , with allowance for sediment inflows from hillslopes. If x is taken as the downslope direction and y as the downstream direction, we have:

$$\frac{\partial z}{\partial t} = U - \frac{1}{w} \frac{\partial (wS_y)}{\partial y} + \frac{2S_x}{w} \quad (5)$$

where S_x and S_y indicate sediment flows in the downslope and downstream directions.

Equation (1), with S_x replacing S remains valid for each hillslope profile, with the basal boundary condition set by the value of $\partial z / \partial t$ for the corresponding point on the stream profile.

Figure 8 illustrates this approach. The stream initially flows for 1000km on a level plateau at 1000m elevation, falling over a steep continental rim to a fixed sea level. Initially identical slope profiles have 100m of relief, in a 200m long hillslope. The figure shows the profiles at 50 Ka. The continental divide shows little lowering, but the stream profile shows the development of a broadly concave profile. The divides show the remains of a summit plateau, which is increasingly incised downstream. Beyond 300km, hillslope relief begins to decline progressively, and the summit envelope mirrors the stream convexity. In the

centre section (300–600km), where relief is greatest, slope profiles are dominated by mass movements. This effect has been widely observed, at a variety of scales (e.g. Carter & Chorley, 1961; Arnett, 1971).

Passive continental margins

For large continental areas, isostatic effects cannot generally be ignored, even if there are no externally imposed tectonic stresses. The section in figure 8 may therefore be seen as representing a passive continental margin, like that around Southern Africa, with offshore sedimentation of eroded material. If it is assumed that the initial uplifted configuration is in equilibrium, and that geothermal gradients are neutral in the sense that loading or unloading will not produce thermal stresses, then erosion and deposition produce a pattern of loading on the elastic lithosphere, which bends in response.

The general equation for two dimensional deflection of a thin elastic plate (Turcotte & Schubert, 1982, Chapter 3) is:

$$D \frac{d^4 w}{dx^4} = q(x) - P \frac{d^2 w}{dx^2} \quad (6)$$

where w is the deflection at distance x along the plate,
 D is the flexural rigidity,
 P is the horizontal force per unit length
and $q(x)$ is the plate loading at x .

Solving for an unbroken continental plate with a point load at $x=0$, the deflection is given by:

$$w = \frac{V_0 \alpha^3}{8D} e^{-\alpha x} \left(\cos \frac{x}{\alpha} + \sin \frac{x}{\alpha} \right)$$

$$\alpha = \left[\frac{4D}{\rho_m g} \right]^{1/4} \quad (7)$$

where V_0 is the point load at $x=0$,
 α is the flexural parameter defined above
and ρ_m is the mantle density.

The equation is the same for the offshore area, but usually with a different flexural rigidity, D , and with the density term replaced by the difference between mantle and water densities. The solution is symmetrical about $x=0$.

For the continuous change in loading associated with erosion, the complete solution is obtained as the sum of a series of terms like Equation (7), displaced with respect to the point of application of the erosional unloading. In the absence of an adequate model for the distribution of offshore deposition, the marine contribution has been approximated as being anti-symmetric with respect to the coastline.

The concentration of both erosion and deposition close to the shoreline lead to massive flexure at the shoreline, with maximum flexural uplift within 200 km of the

coast, and maximum downwarping a similar distance offshore. The example shown in Figure 9 is for a mantle density of 3300 kg m^{-3} and a flexural rigidity modulus of $1.1 \times 10^{24} \text{ Nm}$, which corresponds to a 56km elastic lithosphere thickness and a flexural parameter of 108 km. Isostatic uplift raises the summits, while incision of stream courses more or less keeps pace with the uplift. Slopes therefore become very steep, generating a coastal range of rugged mountains, enclosing a plateau of more moderate relief. The curve for isostatic uplift also shows the warping undergone by originally horizontal strata, which are deformed into outward facing escarpments, with a dip which increases with time. There is scope to measure the cumulative amounts and rates of exhumation associated with this process using methods which include apatite fission track dating (Brown et al, in press) and examination of metamorphic grade.

At many continental margins, the assumption of a neutral geothermal gradient is inappropriate. The continental margin may well be associated with crustal thinning which has strong thermal implications. In addition, the accumulation of sediment offshore may induce thermal stresses which encourage continental growth through uplift and accretion of accumulated offshore sediment.

Conclusions

Although there is scope for much further development of these themes, we have demonstrated the feasibility of extending relatively simple geomorphological process models up to basin or continental scales. It is possible to retain a link with our understanding of small scale process, and to link areas together, essentially using a simplified fluvial transport process at the large scale.

Stream processes appear to dominate at large scales, and many aspects of their behaviour can be approximated as flux limited processes. This approach therefore has some validity, both for the simple one-dimensional envelope profile method and as the linking stream process within a slope/ stream scheme. Its greatest weakness may be for very large rivers, where a high proportion of the alluvial sediment is in silt and finer grain sizes, for which there is no well defined transporting capacity. In such cases it may be necessary to set up an explicitly grainsize selective model.

Where a flux limited approach is valid, it is reasonable to use characteristic forms as the first order model for whole landscape evolution. This approach breaks down, however, where there are anomalous variations in local relief, as for example occur in the example shown in Figure 9 for passive continental margins. For such cases it is important to include a distinct hillslope component, and to recognise that it may be dominated by supply limited mass movement processes which do not lead toward diffusive characteristic forms.

With adequate geomorphological models, we can, for the first time, investigate the links between geophysical and geological processes and landforms at regional to continental scales. It has become clear that these links are strongly interactive, with impacts of erosion and sedimentation on tectonics which significantly influence the rates of geophysical processes. It is vital that geomorphologists contribute their skills to this new understanding, and ensure that measurements of landscape processes are applied in a wider context.

References cited

- Adams, J., 1985. Large scale tectonic geomorphology of the Southern Alps, New Zealand, in Tectonic Geomorphology, ed M. Morisawa & J.T. Hack, Allen & Unwin, Boston, 105-28.
- F. Ahnert, 1970. Functional relationships between denudation, relief and uplift in large, mid-latitude drainage basins. American J. Science, 268, 243-63.
- R.R. Arnett, 1971. Slope form and geomorphological process: an Australian example. in Slopes: form and process (ed D. Brunnsden). Institute of British Geographers, Special Pub. 3, 81-92.
- K.J. Beven & M.J. Kirkby, 1993. Channel Network Hydrology, John Wiley, Chichester, 319pp.
- R.W. Brown, M.A. Summerfield & J.W. Gleadow, in press. The potential of thermochronologic measures of denudation rates in assessing models of long-term landscape development. in Process models and theoretical geomorphology (ed. M.J. Kirkby), John Wiley.
- C.A. Carter & R.J. Chorley, 1961. Early slope development in an expanding stream system. Geological Magazine, 98, 117-30.
- W.M. Davis, 1899. The Geographical Cycle. Geographical Journal 14, 481-504.
- J.A. Jackson, N.J. White, Z. Garfunkel & H. Anderson, 1988. Relations between normal-fault geometry, tilting and vertical motions in extensional terrains: an example from the Southern Gulf of Suez. J. Structural Geology. 10(2), 155-170.
- M.J. Kirkby, 1971. Hillslope process-response models based on the continuity equation. in Slopes: form and process (ed D. Brunnsden). Institute of British Geographers, Special Pub. 3.
- M.J. Kirkby, 1992. An erosion-limited hillslope evolution model. Catena Supp. 23, 157-87.
- M.J. Kirkby, M.R. Leeder, & N.J. White, in press. The erosion of actively extending tilt-blocks: a coupled model for topography and sediment budgets. Tectonics.
- W. Penck, 1924. Die Morphologische Analyse (Morphological Analysis of Landforms). English translation by. Czech & K.C. Boswell, London, 1953.
- S.A. Schumm, 1963. The disparity between present rates of denudation and orogeny. US Geol Survey, Prof. Paper 454-H, 13pp.
- T.R. Smith & F.P. Bretherton, 1972. Stability and the conservation of mass in drainage basin evolution. Water resources Research 8(6), 1506-29.
- D.L. Turcotte & G. Schubert, 1982. Geodynamics: Applications of continuum physics to geological problems, John Wiley, New York, 450pp.
- G.R. Wilgoose, R.L. Bras & I. Rodriguez-Iturbe, 1991. Results from a new model of river basin evolution. Earth Surface Processes & Landforms 16, 237-54.

TABLE 1: File of Slope process rates used for simulations shown in Figure 1 (a)-(c)

SLOPE DIMENSIONS

- 250 Slope length (m)
- 50 Summit Height (m)
- 20 Number of points down slope

PROCESS RATES PARAMETERS:

(i) SOIL CREEP

- 10 Rate (sq.cm/a)
- 1 Creep Travel distance on unit gradient (m)

(ii) SOLUTION (Rate falls in inverse proportion to a/s above critical value given below)

- 20 Rate of Solutional lowering ($\mu\text{m/a}$)
- 100 Soil saturated hydraulic conductivity (m/day)
- 100 Time to reach chemical equilibrium (Hours)
- 100 Soil Residence Time in unsaturated phase (Hours)
- 1000 Critical value of a/Λ (unit area \div gradient in m)

(iii) LANDSLIDES

- 10 Rate of free degradation (mm/y)
- 22 Threshold angle ($^\circ$)
- 35 Talus gradient ($^\circ$)
- 20 Travel distance (m)

(iv) SPLASH

- 1 Rate of Detachment (mm/y)
- 50 Distance (m) for attenuation of detachment by water film per unit gradient
- 1 Travel distance per unit gradient (m)

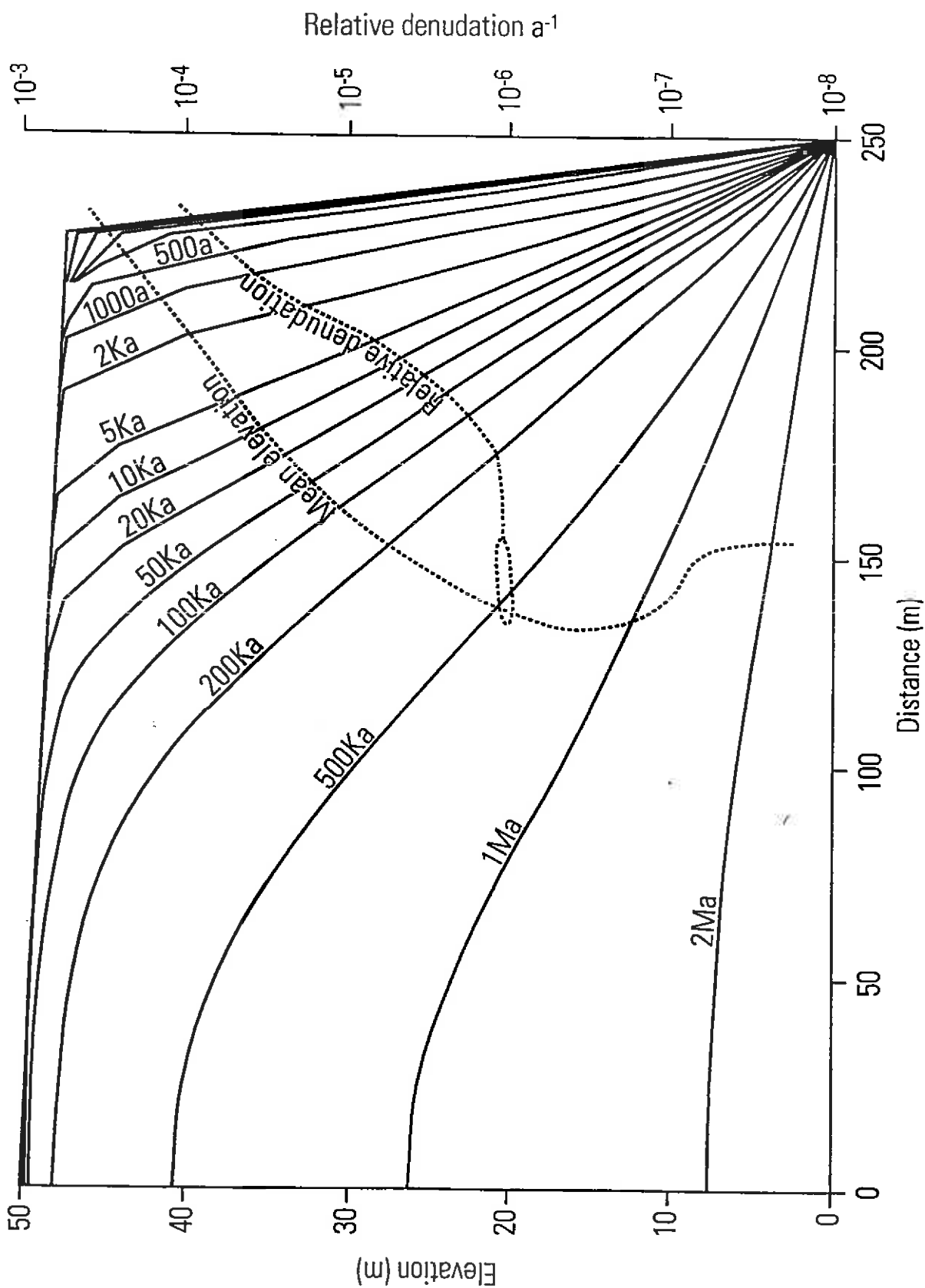
(v) RILLWASH:

- 0.01 Rate of detachment at unit $x \approx \Lambda$ (mm/m.y)
- 0 Detachment threshold (m) per unit gradient
- 0.01 Travel distance per unit distance in flow

curves show evolution over time. Dotted curves show progressive change over time, with x-axis plotted as the ratio or mean elevation to summit elevation (100% at far right). For mean elevation curve, y-axis is absolute mean elevation. For relative denudation curve, y-axis is the mean rate of denudation divided by the mean elevation, plotted to the logarithmic scale at the right. The three examples differ only in the (constant) rate of downcutting applied at the slope base.

- (a) with fixed basal elevation
- (b) Constant lowering at $50 \mu\text{m a}^{-1}$
- (c) Constant lowering at $100 \mu\text{m a}^{-1}$

In (b) and (c), the broken lines show the equilibrium profile form.



basal position. Solid curves show evolution over time. Dotted curves show progressive change over time, with x-axis plotted as the ratio of mean elevation to summit elevation (100% at far right). For mean elevation curve, y-axis is absolute mean elevation. For relative denudation curve, y-axis is the mean rate of denudation divided by the mean elevation, plotted to the logarithmic scale at the right. The three examples differ only in the (constant) rate of downcutting applied at the slope base.

(a) with fixed basal elevation
 (b) Constant lowering at $50 \mu\text{m a}^{-1}$
 (c) Constant lowering at $100 \mu\text{m a}^{-1}$

In (b) and (c), the broken lines show the equilibrium profile form.

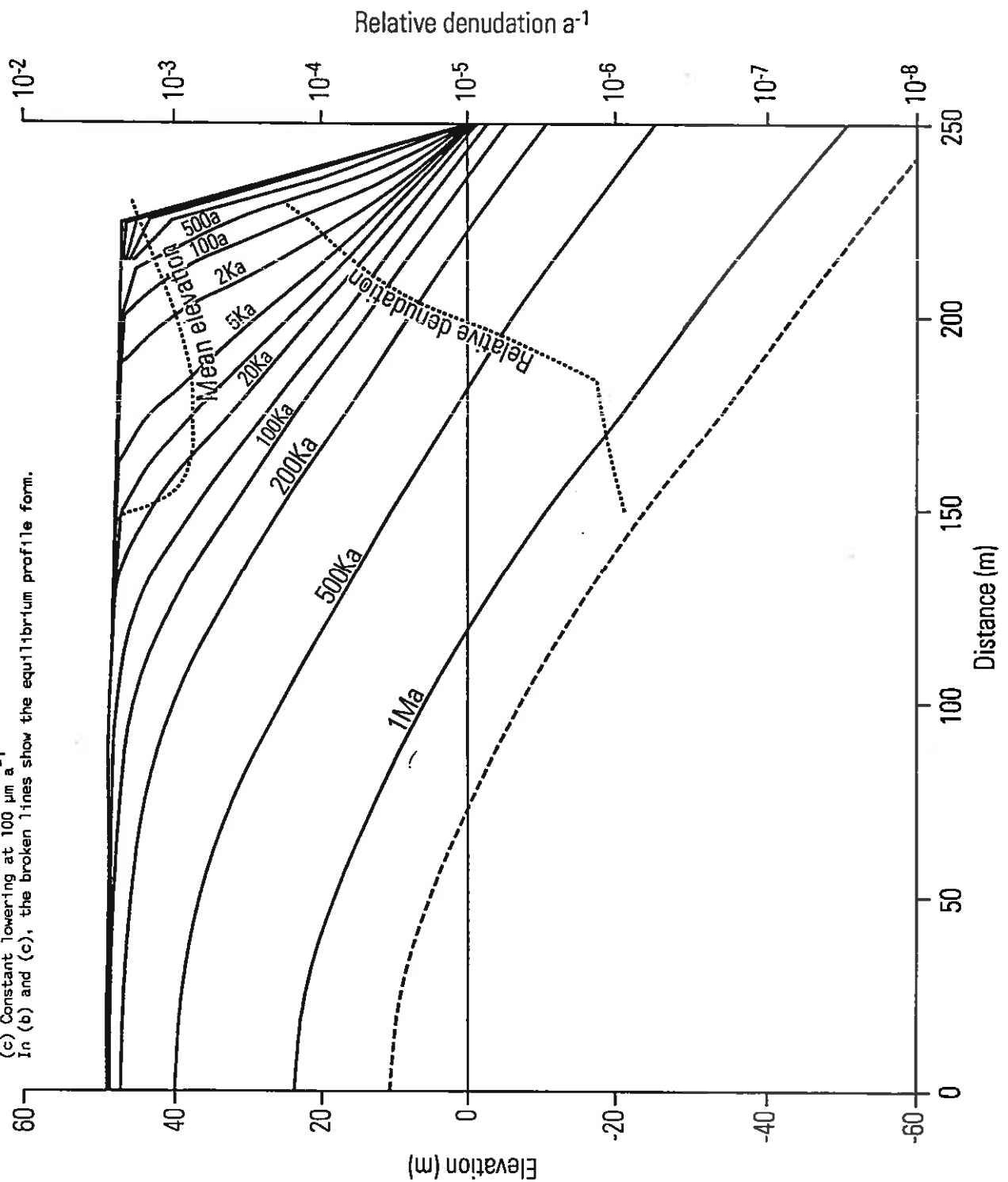


Figure 1c In all cases the initial form is a gently sloping plateau, bounded by a cliff which falls to a fixed basal position. Solid curves show evolution over time. Dotted curves show progressive change over time, with x-axis plotted as the ratio of mean elevation to summit elevation (100% at far right). For mean elevation curve, y-axis is absolute mean elevation. For relative denudation curve, y-axis is the mean rate of denudation divided by the mean elevation, plotted to the logarithmic scale at the right. The three examples differ only in the (constant) rate of downcutting applied at the slope base.

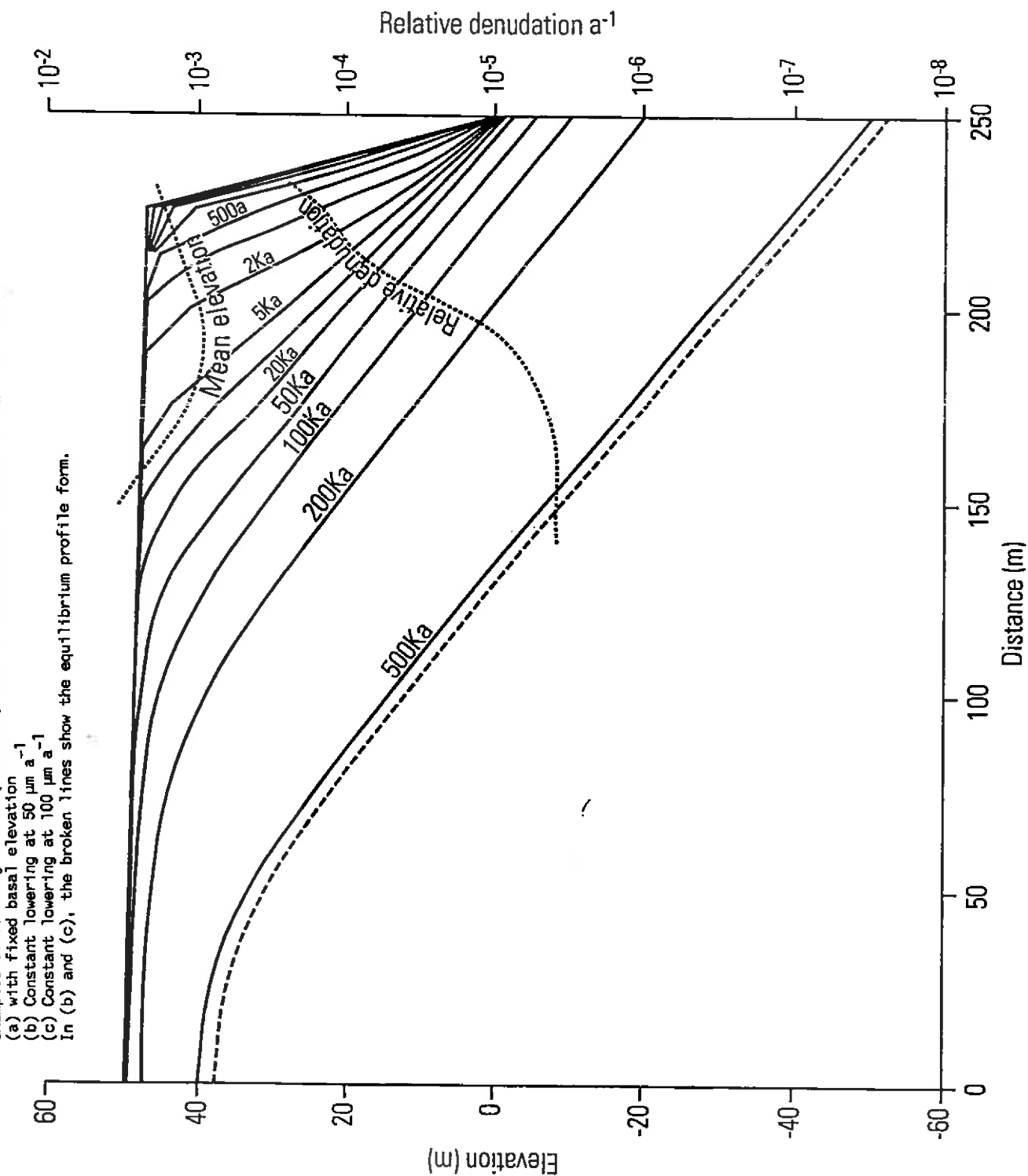


Figure 2: Final equilibrium relative denudation rates (Mean denudation rate divided by mean profile relief) expressed in terms of steady state basal downcutting rates, for a series of profile sequences including those shown in figure 1.

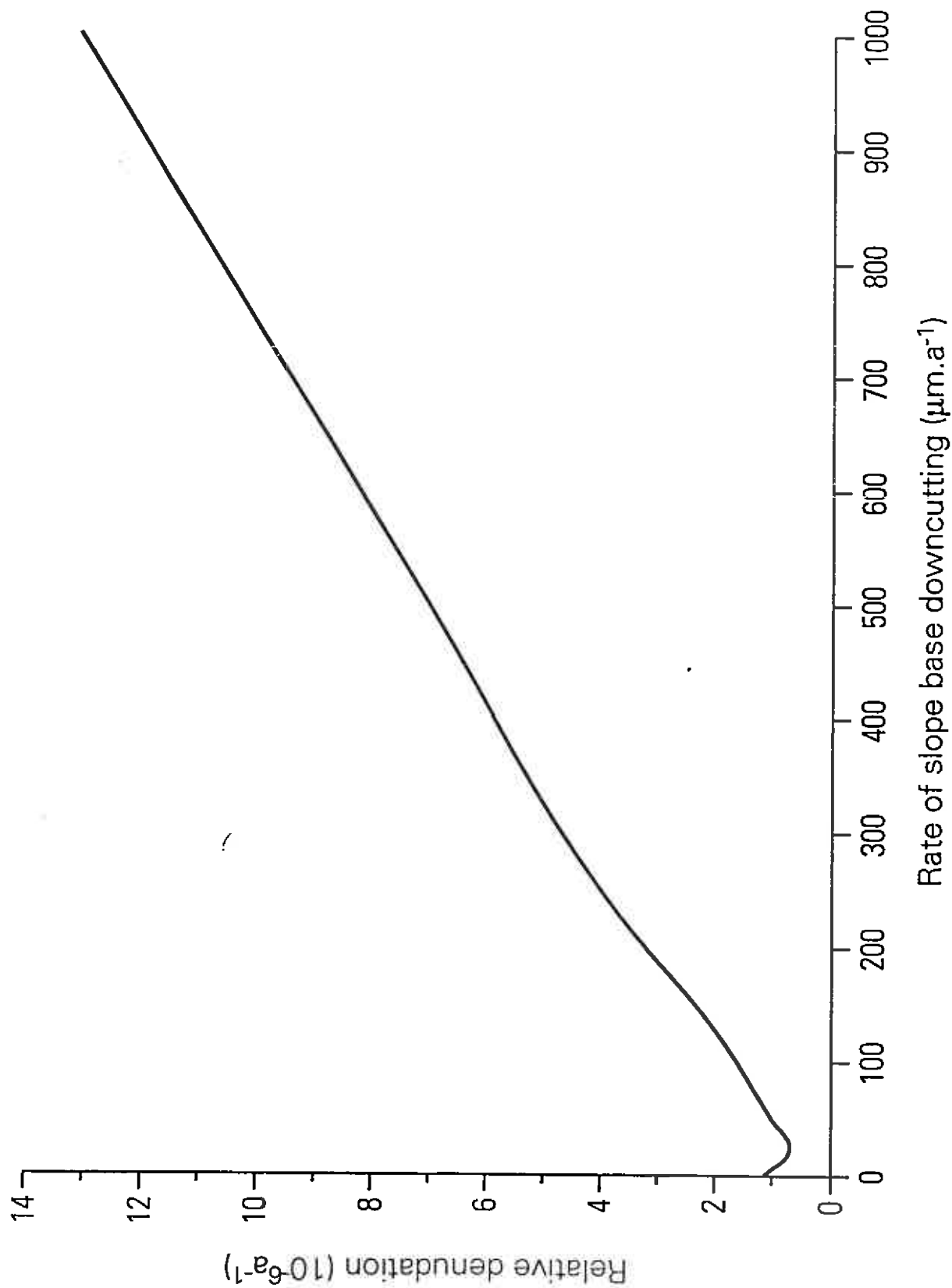


Figure 3: Profiles in equilibrium with differing rates of constant downcutting, for a combination of diffusive processes (splash, creep, solifluxion) and mass movements. Profiles are shown as logarithmic plots of gradient against distance from the divide. Rates are as shown in Table 1.

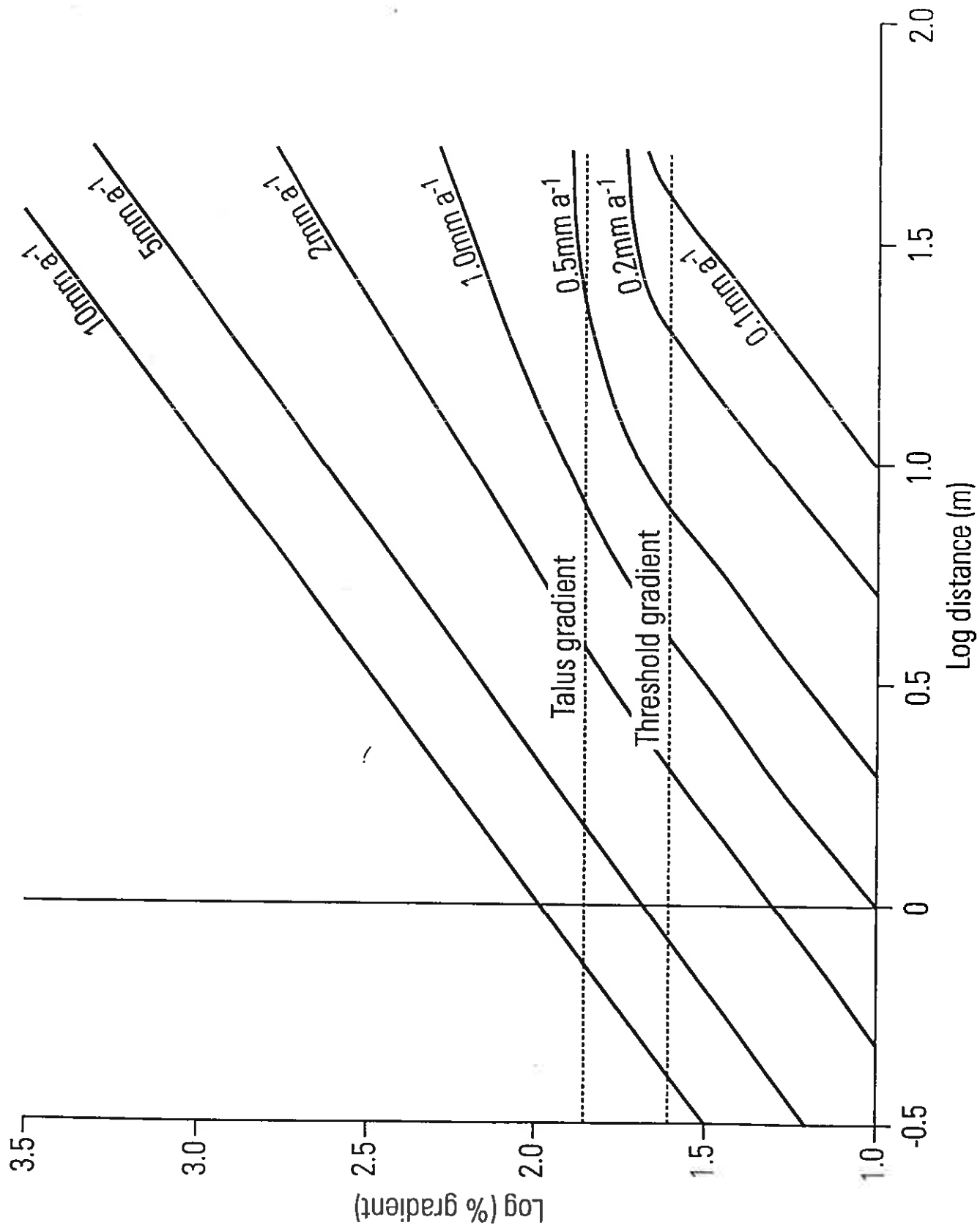


Figure 4: Schematic relationship between long term rate of relative denudation (β) and tectonic uplift rate. Some mass movement activity is assumed in addition to diffusive processes (splash, creep and wash). Relative denudation is expressed in terms of steady uplift rate and climate. Lithology influences the relationship primarily through its impact on mass movement rates.

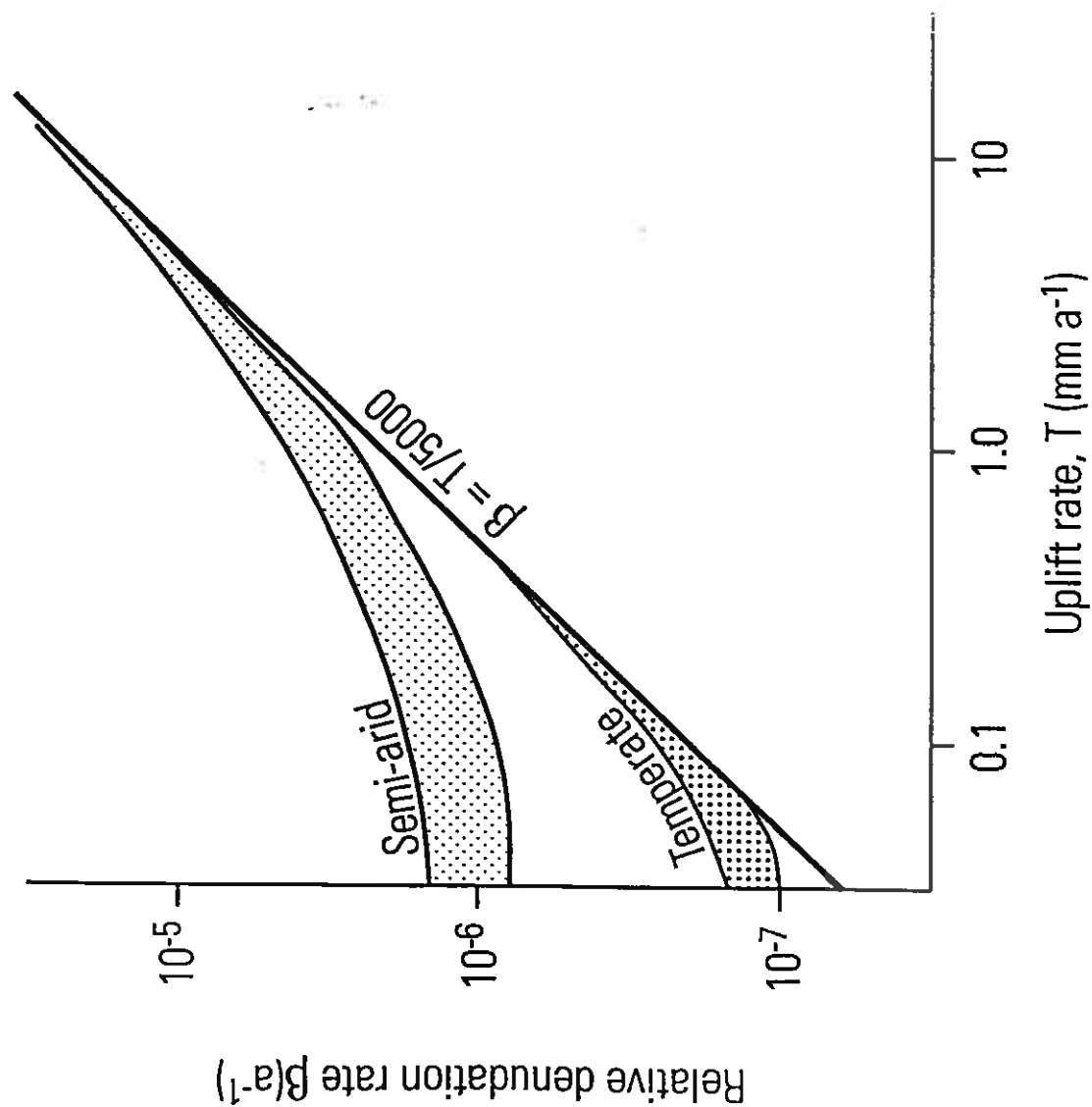


Figure 5: Cartoon showing equilibrium landforms associated with domino block extensional faulting. Upper lines show block fault structures. Centre curve shows equilibrium profile for a closed sedimentary basin in balance with faulting. Note modest basin asymmetry, and summits substantially displaced from the fault lines. Lower lines show resulting equilibrium rates of uplift or lowering.

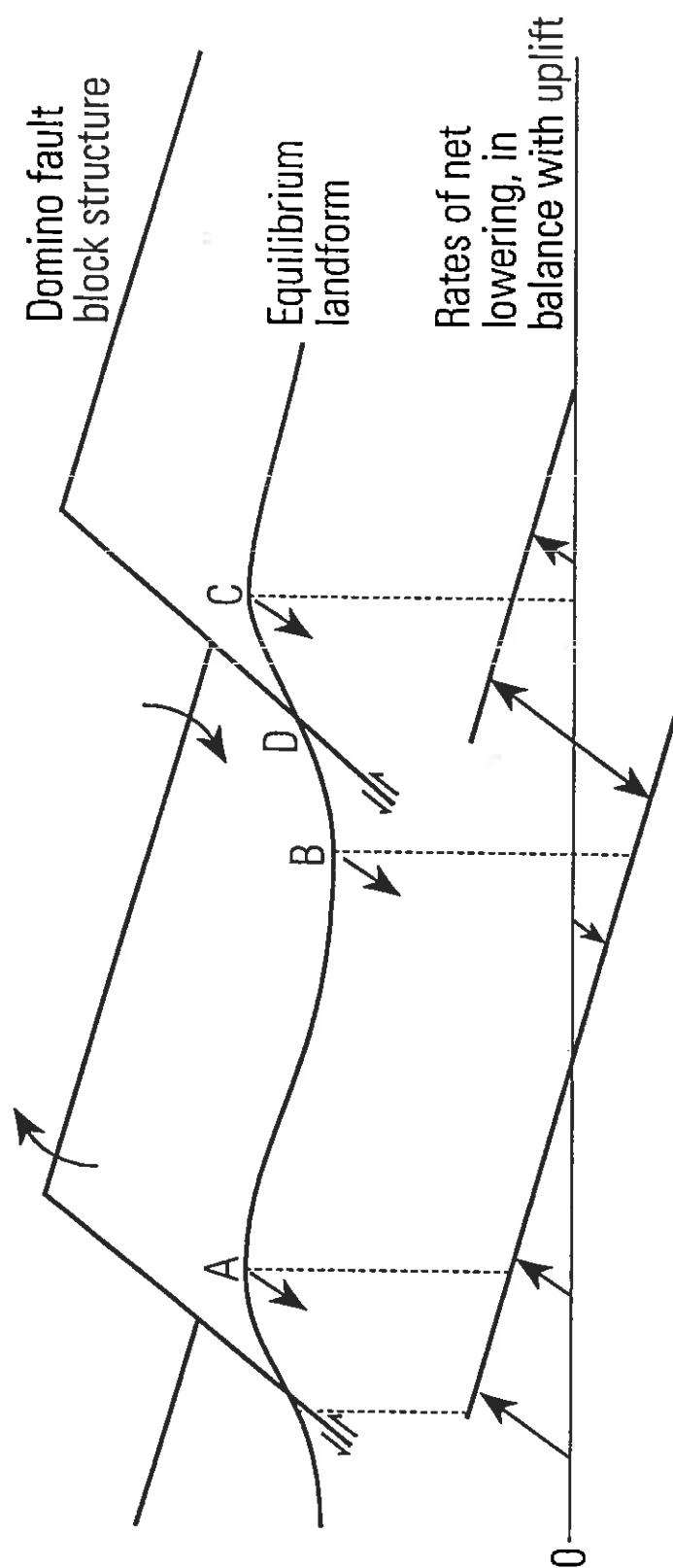
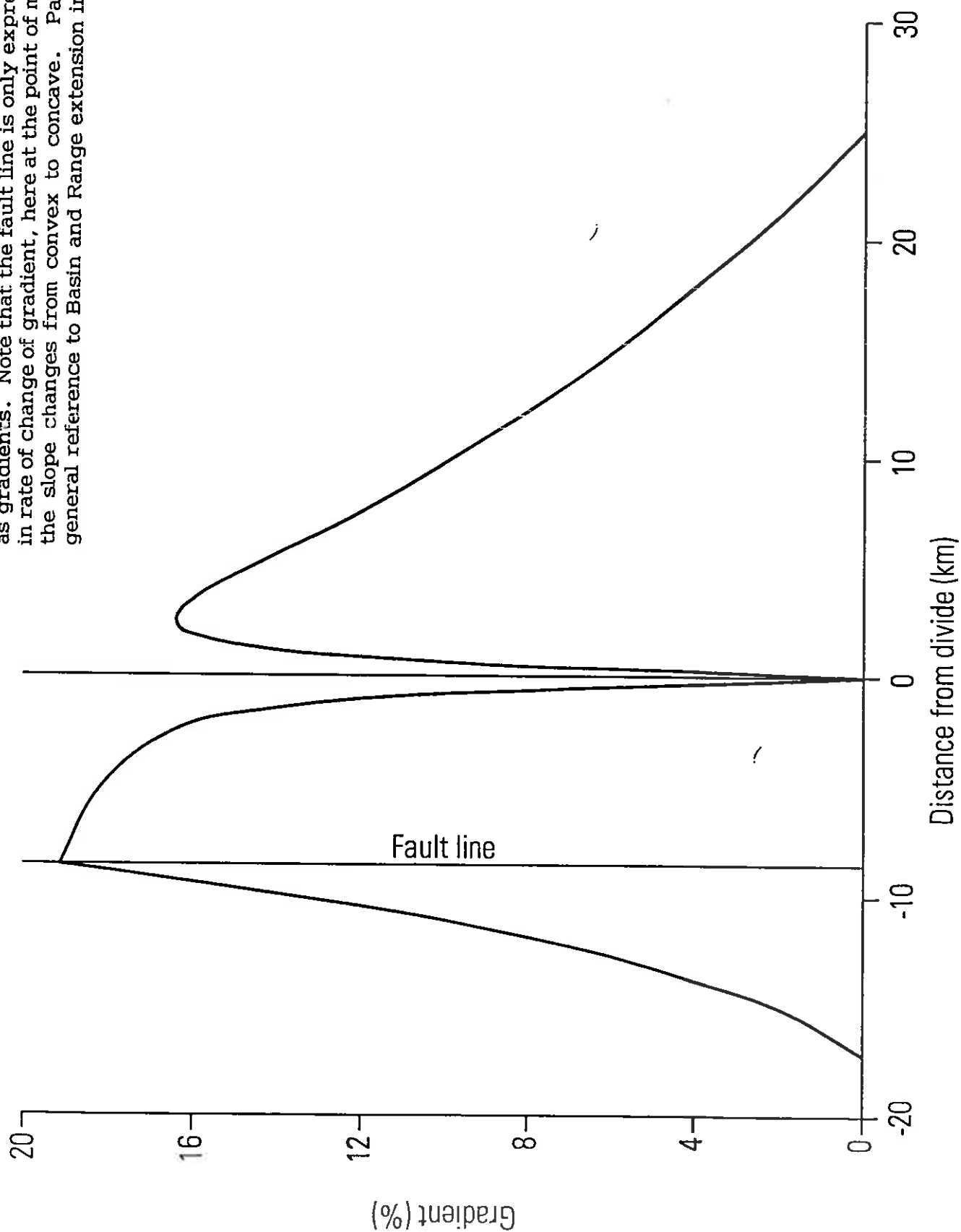


Figure 6: Example equilibrium profile obtained for a closed continental basin, in balance with block faulting as outlined in figure 6. Profiles are expressed as gradients. Note that the fault line is only expressed as a discontinuity in rate of change of gradient, here at the point of maximum gradient where the slope changes from convex to concave. Parameters selected with general reference to Basin and Range extension in Nevada.



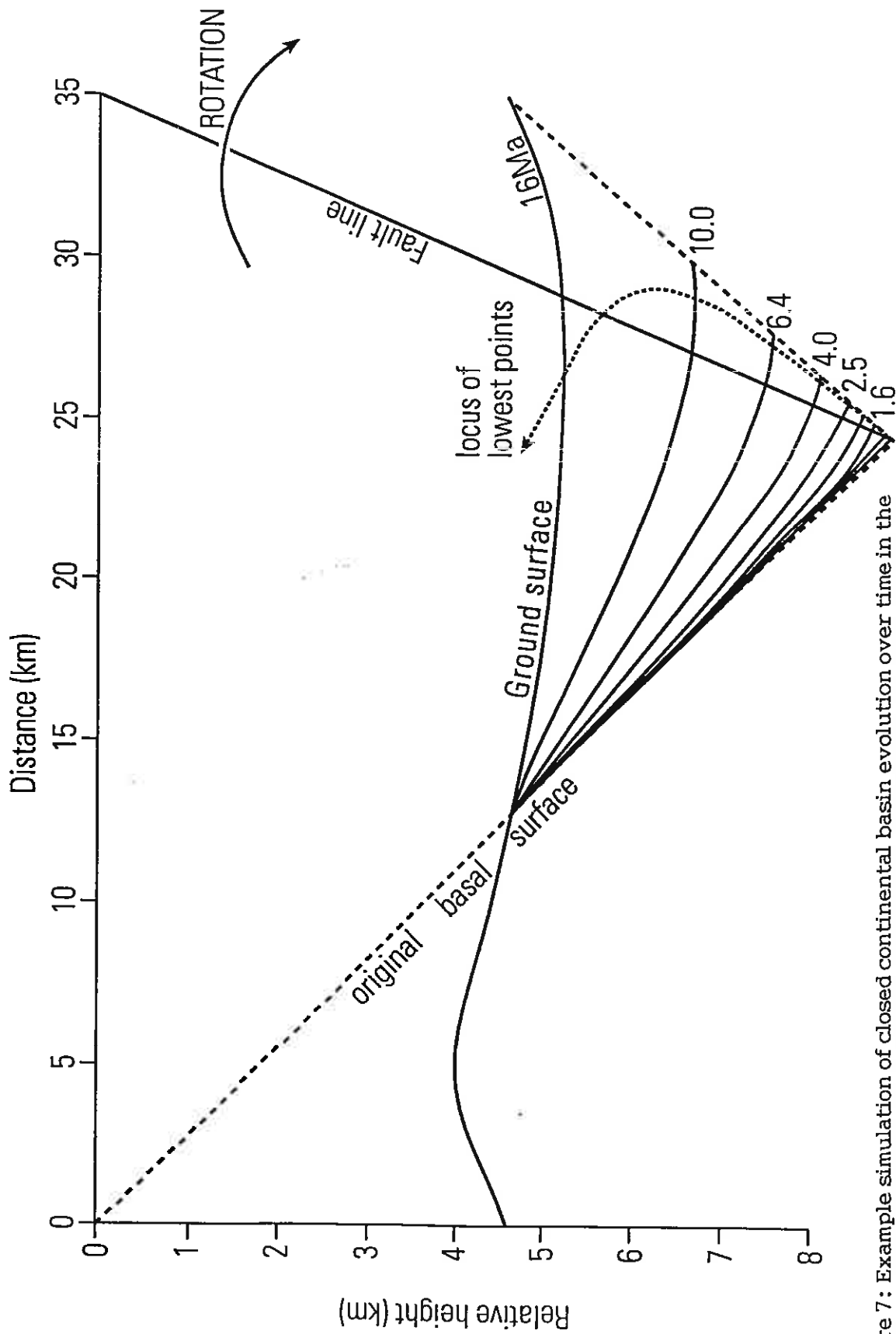


Figure 7: Example simulation of closed continental basin evolution over time in the presence of extensional domino block faulting. Parameters are chosen for the Dixie Valley/ Clain Alpine Range, Nevada. Solid lines show successive isochrons for basin fill over basal basalt flows. Note the position of the main fault line well within the basin sediments, and the modest topographic asymmetry of the basin (from Kirkby & Leeder, 1993?).

initially with 100m of relief, with no tectonic effects. Curves falling from left to right show the mainstream and summit envelope profiles, and the hillslope relief. Curves falling from right to left show 10 constituent slope profiles.

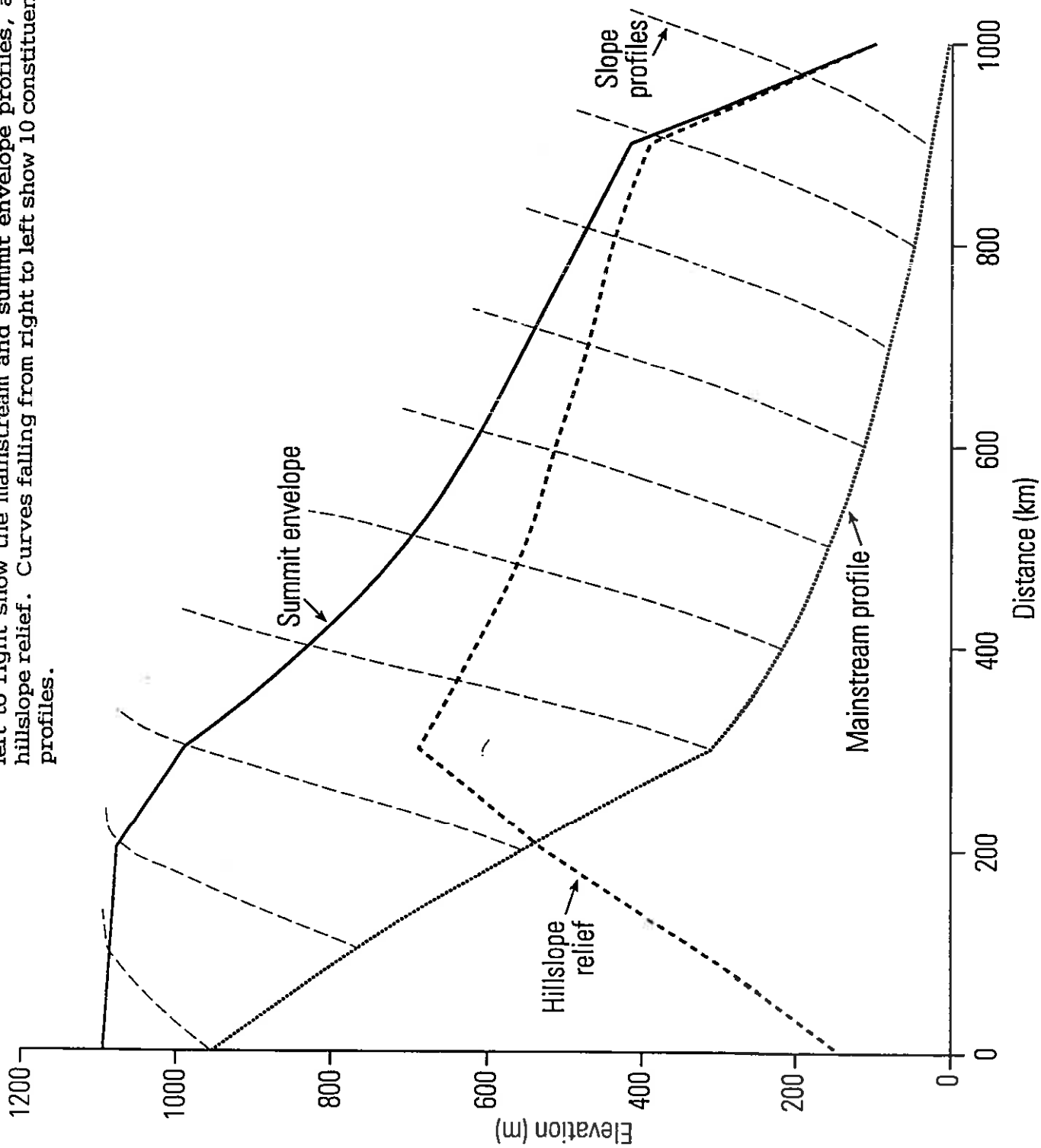


Figure 9: Illustration of stream/slope profiles for same process rates and notation as in Figure 5 above. Profiles here represent a passive continental margin, with no external tectonics, but with isostatic uplift, and flexure using average parameters (Turcotte & Schubert, 1982, Chapter 3) for continental elastic response. For simplicity, offshore response to sediment loading and flexure is assumed anti-symmetric about the shoreline. Note the evolution of a coastal mountain range with very steep side-slopes, and the folding of initially horizontal strata with the isostatic uplift to generate shoreline-facing escarpments.

